Optoacoustic sensing of hematocrit to improve the accuracy of hybrid fluorescence-ultrasound intravascular imaging

Dmitry Bozhko,[1,2], Angelos Karlas[1,2], Dimitris Gorpas[1,2] and Vasilis Ntziachristos[1,2,]*

*Corresponding Author: E-mail: v.ntziachristos@tum.de

[1] Institute of Biological and Medical Imaging, Helmholtz Zentrum München, Neuherberg, 85764 Germany

[2] Chair of Biological Imaging, Technische Universität München, Munich, 85764 Germany

Keywords: Intravascular Ultrasound, Photoacoustic, Near-infrared Fluorescence, Quantitative Imaging, Multimodal Imaging

Short title: D. Bozhko et al.: Optoacoustic sensing of hematocrit to improve NIRF-IVUS imaging

Hybrid intravascular fluorescence-ultrasound imaging is emerging for reading anatomical and biological information *in vivo*. By operating through blood, intravascular near-infrared fluorescence (NIRF) detection is affected by hemoglobin attenuation. Improved quantification has been demonstrated with methods that correct for the attenuation of the optical signal as it propagates through blood. These methods assume an attenuation coefficient for blood and measure the distance between detector and the vessel wall by observing the intravascular ultrasound (IVUS) images. Assumptions behind the attenuation employed in correction models may reduce the accuracy of these methods. Herein, we explore a novel approach to dynamically estimate optical absorption by using optoacoustic (photoacoustic) measurements. Adaptive correction is based on a tri-modal intravascular catheter that integrates fluorescence, ultrasound and optoacoustic measurements. Using the novel catheter, we show how optoacoustic measurements can determine variations of blood absorption, leading to accurate quantification of the detected NIRF signals at different hematocrit values.

This article has been accepted for publication and undergone full peer review but has not been through the copyediting, typesetting, pagination and proofreading process, which may lead to differences between this version and the Version of Record. Please cite this article as doi: 10.1002/jbio.201700255

1. Introduction

Hybrid intravascular fluorescence – ultrasound imaging systems add pathophysiology readings to stand-alone intravascular ultrasound (IVUS) by employing fluorescence agents tuned to specific biological parameters of interest. When near-infrared fluorescence (NIRF) is used, through-blood detection can be achieved due to the low light attenuation by blood in the near-infrared spectral region. The development of hybrid NIRF-IVUS catheter systems for *in vivo* imaging was recently demonstrated, allowing detection of multiple atheroma-related pathophysiological parameters including plaque formation, [1] protease activity,[2–5] oxidized low-density lipoprotein content,[6] plaque permeability,[1,3] as well as fibrin deposition on coronary stents.[3]

Despite the demonstrated promise, a challenge in NIRF-IVUS imaging is the accurate quantification of the fluorophore concentration in the vessel wall. Quantification of NIRF readings may be limited by variations in the fluorescence signal during vessel examination due to (1) varying distance between the vessel wall and the fluorescence detector on the distal end of the catheter, and (2) light attenuation by blood, the magnitude of which is unknown. Both parameters affect NIRF readouts during "pullback", when the catheter is pulled through the lumen while acquiring data. These factors may affect the fluorescence signal independently of the underlying fluorophore concentration, leading to inaccurate representation of fluorophore concentration and false characterization of the vessel wall and plaque condition.

It was previously demonstrated that IVUS images can be employed to improve the accuracy of intravascular NIRF by providing information on the wall-catheter distance throughout the blood vessel.[7,8] This information can then be used to establish a distance correction model for measurements through blood *in vivo* and thereby correct for fluorescence intensity variations, assuming the blood attenuation is known.[1,3,9] However, blood attenuation usually remains unknown during *in vivo* measurements, hindering the establishment

of an accurate personalized correction model. We have previously determined that blood attenuation *in vivo* differs significantly from that *ex vivo*,[3] and that using *ex vivo* value does not lead to accurate signal quantification. Overall, knowledge of the exact light-attenuation parameters during the measurement are required for precise IVUS-based correction of NIRF data.

Current fluorescence correction algorithms for NIRF-IVUS applications compensate for distance-related attenuation by approximating light attenuation based on the Beer-Lambert law using blood absorption parameters extracted from the literature or Monte Carlo simulations.[1] Empirical models based on *ex vivo* or *in vivo* measurements of blood attenuation in phantoms have also been considered.[3,9] These empirical and theoretical approaches use fixed attenuation models that ignore variation in blood optical properties between pullbacks and between patients. To make NIRF-IVUS technology applicable for clinical use, novel attenuation models are needed that feature increased adaptability to the varying optical properties of surrounding media on a per-case basis.

In this study, we aimed to develop a method that could dynamically track the blood attenuation during each measurement *in vivo*. To achieve this, we hypothesized that the addition of optoacoustic measurements as a third modality to the hybrid NIRF-IVUS catheter could detect hemoglobin absorption based on hematocrit changes and enhance the correction model employed. Therefore, in contrast to previous intravascular optoacoustic systems,[10–15] we employed optoacoustic signal originated from blood surrounding catheter. To examine our hypothesis, we developed a tri-modal catheter system and applied it to measurements of phantoms and tissues. We further developed a method that relates the optoacoustic data to the attenuation characteristics of blood and integrates them into a NIRF correction model for intravascular applications. We then evaluated the proposed model under clinically relevant scenarios in which fluorescent dye accumulation inside a vessel wall was quantitatively assessed through blood at varying hematocrit levels.

2. Materials and Methods

2.1. Development of a tri-modal NIRF-IVUS-optoacoustic catheter

A NIRF-IVUS system previously developed in our laboratory[3] was adapted with the capability to perform optoacoustic measurements. The original NIRF-IVUS system consisted of two major modules: a rotating intravascular NIRF-IVUS catheter and a stationary back-end console. The catheter utilized a 200-μm core multi-mode (MM) side-firing fiber for NIRF measurements (Precision Optics Corporation, Gardner, MA USA); an IVUS transducer was integrated with the fiber for ultrasound imaging. The back-end console consisted of a continuous-wave (CW) laser source at 670 nm (B&W Tek, Lübeck, Germany) for NIRF excitation and a pulser-receiver (Olympus 5073PR, Hamburg, Germany) to drive the ultrasound transducer. During pullback, the hybrid catheter was rotated and translated inside a sealed water-filled plastic sheath using two programmable motorized stages. Based on our previous work using IVUS transducers with central frequencies of 15 or 40 MHz,[3] we used the 9F/15MHz transducer for the current study (Boston Scientific, MA, USA).

The optoacoustic modality in our tri-modal system was implemented with a pulsed laser source illuminating at 515 nm (Flare HP PQ Green 2k-500, Innolight, Suzhou, Jiangsu, China) with a repetition rate of 1.2 kHz (**Figure 1**). Laser light was co-aligned with the NIRF beam using a dichroic mirror with a cut-off wavelength of 638 nm in a free-space arrangement, and the two beams were coupled into the same fiber of the imaging catheter. IVUS detector and optical fiber were aligned so that the fields of optoacoustic excitation and ultrasound detection overlapped at radial distances of 0.6-2.7 mm, providing maximum optoacoustic sensitivity at 1.1 mm from the detector. IVUS and optoacoustic signals were separated in the time domain using a custom-built triggering device. To allow more light from the free-space arrangement into the fiber, the core diameter of the side-firing MM fiber of the tri-modal imaging catheter

was increased from 200 μm as in the original NIRF-IVUS system[3] to 400 μm. This allowed delivery of higher optical power for optoacoustic excitation of the tissue. As a result, from 40mW output laser power at 515 nm, 16.7 mW was measured at the tip of the catheter (13.9 μJ pulse energy, 42% coupling efficiency). For CW laser at 670 nm, from 35.8 mW laser output, 24 mW was exiting the catheter (67% coupling efficiency). It should be noted however, that use of a MM fiber with a bigger core compromised NIRF resolution. For imaging range of 0.6-2.7 mm we calculated the beam diameter to double when 400 μm core fiber is used instead of a 200 μm core fiber.

During pullback, 3000 A-lines were measured per rotation, resulting in a frame rate of 0.5 Hz and pullback speed of 0.25 mm/sec. Each set of 100 consecutive optoacoustic A-lines was averaged to eliminate the effects of pulse-to-pulse energy fluctuations. Then IVUS and optoacoustic data were bandpass-filtered (10-20 MHz) to improve the signal-to-noise ratio, Hilbert-transformed, and arranged into a set of cross-sectional B-scans. IVUS images were manually segmented to allow estimation of the distance between catheter tip and sample. Optoacoustic signals were analyzed to find the maximal amplitude, and this value was related to the hematocrit of the surrounding blood (see next section). Finally, each IVUS B-scan was transformed from polar to Cartesian coordinates. NIRF signals were first filtered with a low pass filter and then plotted in two-dimensional images in which the horizontal axis showed the rotation angle and the vertical axis showed the pullback position relative to the starting scanning point.

2.2. Development of the blood attenuation model

Detected NIRF intensity is influenced by three main parameters: (1) the fluorophore concentration, (2) the distance of light propagation in blood, and (3) the blood attenuation. We compiled these parameters into a comprehensive attenuation model in the form of a four-

dimensional look-up table, so that NIRF data could be represented in quantitative units of fluorophore concentration.

To compile the attenuation model, we first assumed a linear relationship between NIRF intensity and fluorophore concentration.[16] Then we employed the Twersky theory[17] to model the attenuation of light with distance using a two-term exponential function. Finally, we added an adaptive attenuation term to account for variations in hematocrit and therefore for corresponding variations in light attenuation by blood. Hematocrit variations affect both light absorption (by altering the hemoglobin concentration) as well as light scatter (by altering the number of blood cells). We hypothesized that measurements of optoacoustic signals could track these changes and thereby allow adjustment of the adaptive attenuation term. While a quantitative optoacoustic inversion formula has previously been introduced to predict optoacoustic signals generated by a point source,[18] the inversion of single point measurements poses a mathematical problem without a unique solution. Therefore, we determined experimentally the relationship between hematocrit and detected optoacoustic amplitude.

As a result, the developed attenuation model included a set of distance correction look up-tables specific for blood hematocrit. The appropriate look-up table to be used for correction of data from each pullback was selected based on optoacoustic amplitude.

3. Experimental

To validate both the tri-modal system and proposed correction model we performed three experiments.

Experiment 1 was performed to calibrate the blood attenuation model. Therefore, we measured NIRF-IVUS-optoacoustic signals during scan of a transparent polymeric tube filled with fluorescent dye AlexaFluor® 680 (200 mg/ml, Ex./Em. 679/702 nm) and submerged in blood with different levels of hematocrit. The tube lay at an angle of approximately 30° relative

to the catheter. Blood obtained from a healthy White New Zealand rabbit was diluted with normal saline to hematocrit levels of 10, 20 and 30%, with undiluted blood assumed to have a hematocrit of about 40%.[19,20] Distilled water was used to model a hematocrit of 0. NIRF signal from the phantom was measured during each pullback, while distances from catheter to phantom were extracted from IVUS data. Simultaneously, optoacoustic signal generated by surrounding blood was recorded. Then, for each pullback, known hematocrit level was empirically related to the maximum optoacoustic amplitude. Maximum value over the pullback was used to eliminated rotational variations. Then, all four parameters of NIRF intensity, distance, optoacoustic amplitude, and fluorophore concentration were compiled into a comprehensive look-up table that would serve as the attenuation correction model.

In Experiment 2 the model was validated using a new fluorescence tube phantom filled with AlexaFluor® 680 (200 mg/ml) and submerged in rabbit blood diluted to an assumed hematocrit of 30%. The catheter was pulled back for a distance of 22 mm, during which NIRF, IVUS and optoacoustic signals were recorded. Distances between the imaging catheter and the tube phantom were extracted from IVUS data at every pullback position. Hematocrit was determined based on the maximal optoacoustic amplitude as described above, and NIRF measurements were corrected using the blood attenuation model.

In Experiment 3 the model was validated using a biological phantom based on excised tissue. A 33-mm long section of an abdominal aorta was obtained from a healthy White New Zealand rabbit. We injected AlexaFluor® 680 (200 mg/ml) at three locations (0.2 ml each) into the outer layer of rabbit abdominal aorta *ex vivo*. The arterial section was submerged into rabbit blood diluted to an assumed hematocrit of 30% and scanned using the tri-modal catheter. NIRF signals were corrected using the blood attenuation model.

Overall, optoacoustic measurements were repeated 4-6 times at each level of hematocrit. For reproducibility assessment standard deviation between measurements, including phantom experiments and ex vivo imaging, was calculated.

4. Results

Figure 2a depicts the dimensionality of the model, which correlates NIRF signal amplitudes to three independent parameters: fluorophore concentration, distance between the catheter tip and fluorescent target (determined from co-registered IVUS data), and optoacoustic amplitude. **Figure 2b** shows that, based on data obtained with the fluorescent phantom, NIRF signal dropped exponentially with distance, and this drop became steeper as hematocrit increased. As per Twersky theory,[17] we fitted experimental data with a two-term exponential functions. **Figure 2c** depicts the relationship between optoacoustic amplitude and hematocrit. Measured data could be fitted with an exponential function (red line) with $R^2 = 0.997$. All fitting parameters are accessible in Supplemental Material. The relationship between optoacoustic amplitude and hematocrit was combined with a distance correction function to adjust the NIRF signal. The resulting model would allow NIRF measurements taken at a given distance-to-target (determined from IVUS data) and a given hematocrit (determined from optoacoustic amplitude) to be converted into absolute fluorophore concentration.

Next, in Experiment 2 we tested whether this blood attenuation model could recover the correct fluorophore concentration during pullback scanning of a tube phantom in blood with a hematocrit of 30%. **Figure 3a** shows the experimentally measured NIRF intensity along the fluorescent tube. The maximal optoacoustic signal was 5.7 mV, corresponding to a hematocrit of 26.7%, which differs by only 3.3% from the actual value of 30%. **Figure 3b** shows NIRF intensity following attenuation correction based only on distance-to-target, with hematocrit simply assumed to be that of pure blood (40%).[19] **Figure 3c** shows NIRF intensity along the tube, following correction for blood attenuation based on both the IVUS-derived distance-to-

target as well as the optoacoustically measured hematocrit. This dual correction resulted in the most accurate representation of constant fluorophore concentration in the tube over the pullback, highlighting the importance of correcting for hematocrit. **Figure 3d** confirms the importance of correcting for both distance and hematocrit: applying both types of correction yielded the correct fluorophore concentration of 200 mg/ml, which remained roughly constant throughout the pullback. Nevertheless, the error in concentration estimation increased with longer distance, from 10 mg/ml (5%) at a distance of 0.5 mm, to 24 mg/ml (12%) at a distance of 1.9 mm. This suggests that correction errors increase with distance. Hematocrit calibration was critical for accuracy: without it, the correction algorithm overestimated blood attenuation, giving fluorophore concentration values up to 4-fold greater than the actual value.

Following validation with a tube phantom, in Experiment 3 we tested the blood attenuation model for *ex vivo* imaging of rabbit abdominal aorta. **Figure 4a** shows a representative tri-modal cross-sectional image, in which the IVUS image appears in black-and-white, the optoacoustic image appears as a black-red-yellow (hot) colormap, and the NIRF signal encircles the entire image as a ring. Inset depicts optoacoustic maximum intensity projection (MIP) over the pullback. Blue and green circles outline optoacoustic focal range 0.95-1.3 mm. Hematocrit was estimated to be 28.4%, which differs by 5.3% from the known value of 30%. Distances from the target were extracted from manually segmented IVUS images and input in the blood attenuation model to retrieve the fluorophore concentration inside the vessel wall. **Figure 4b and c** demonstrates the distance-corrected NIRF imaging without and with hematocrit calibration, correspondingly. **Figure 4d** shows that, as with the fluorescent tube phantom, the distance correction with hematocrit calibration was essential for obtaining reasonable estimates of fluorophore concentration (red curve). In contrast, correcting NIRF signal based only on distance led to overestimation of blood attenuation and physically impossible concentrations above the maximum of 200 mg/ml (green curve). Correcting the

signal for distance and calibrating for hematocrit gave a maximum concentration of 115.9 mg/ml, which is consistent with expected fluorophore diffusion from the sites of injection.

5. Discussion.

NIRF-IVUS shows potential for visualizing a wider range of physiological and pathophysiological features of tissue *in vivo* than either modality on its own. While ultrasound reveals intravascular morphology, it is not effective at resolving plaque composition or biological processes associated with the vessel wall or potentially with plaque vulnerability. NIRF complements these deficiencies by enabling high-resolution molecular imaging, but fluorescence detection through blood requires attenuation correction. Therefore, two parameters must be known: (1) the distance between the fluorescence detector in the catheter tip and the vessel wall, which can be obtained from the ultrasound images; and (2) the absorption of the NIRF signal by blood. While several methods have been developed to correct NIRF signals based on distance, we are unaware of methods taking into account variations in blood attenuation.

Here we describe a novel approach in which optoacoustic signal is used to estimate hematocrit, which is the major determinant of light absorption and scattering in blood and may vary from patient to patient. Therefore, experimentally determined attenuation models need to be adapted on a per-patient basis for accurate correction that corresponds to the conditions of the blood in the vessel measured. The hematocrit calibration developed here exploits the sensitivity of optoacoustics to haemoglobin,[21–23] measurement of which is used to adjust blood attenuation for each pullback individually. Validation of this blood attenuation model using fluorescent phantoms and rabbit aorta *ex vivo* suggests a model that can allow accurate retrieval of fluorophore concentrations over catheter tip-target distances of up to 2 mm in the presence of blood with hematocrit ranging from 0 (water) to 40% (undiluted blood). This

approach has led to the design of the NIRF-IVUS-optoacoustic catheter, in which the three imaging modalities operate in a perfectly simultaneous and co-registered way to provide more accurate fluorescence-ultrasound images.

The blood attenuation model presented herein comprises two steps: (1) hematocrit calibration and (2) distance correction. The hematocrit calibration occurs based on optoacoustic amplitude detected throughout pullback. This value is associated with a specific hematocrit level and NIRF correction function using a relationship determined experimentally with phantoms. The second step of the blood attenuation model is distance correction, which adjusts for increasing attenuation of the NIRF signal as the photons pass through a longer distance of the scattering medium of blood. Several correction algorithms have been proposed previously, and they differ primarily in where they obtain blood attenuation parameters. In all cases, those algorithms derive distances from IVUS images co-registered with the NIRF images. Our algorithm also takes distances from IVUS images, but it works slightly differently than previous approaches because it re-defines the correction model for each pullback individually based on absorption parameters of surrounding blood measured during the first step of correction. This is, to our knowledge, the first report of correcting NIRF imaging data based on hematocrit, and this calibration is performed using perfectly co-registered optoacoustic, IVUS and NIRF data from the same tri-modal catheter.

Despite only hematocrit was used to modulate optical properties of blood herein, proposed method is sensitive to changes in absorption/scattering of any origin. In clinical settings, optical parameters of blood could also change based on oxygen saturation, cholesterol level, haemolysis, blood velocity, etc.[24] Nevertheless, these changes will correspondingly effect optoacoustic amplitude and therefore will be considered. Additionally, blood attenuation can be defined individually per 2-3 mm segments of the vessel to account for variable blood attenuation due to velocity variations in case of significant stenosis.[25]

This also appears to be the first time that absolute optoacoustic signals have been used to quantify biological parameters in the intravascular environment. Normally, optoacoustic-based intravascular imaging at a single wavelength relies on the time delay between consecutive laser absorption events,[10,11,14,15] while imaging at multiple wavelengths relies on relative – not absolute – amplitudes.[12,13] In the present work, the optoacoustic modality is used to correct the NIRF signal from a NIRF-IVUS-optoacoustic catheter according to a fundamental biological parameter of the surrounding blood: hematocrit. This highlights the flexibility of optoacoustics to support and extend intravascular imaging as either stand-alone or supporting technology.

The model described herein was developed and validated for the fluorescent dye AlexaFluor® 680. It will likely need to be calibrated for each fluorescent dye and detection system individually in order to account for different quantum yields, excitation-emission wavelengths and system sensitivity. This should not pose a problem, given the limited number of fluorescence dyes widely used *in vivo*.[26] Calibration can be done by single measurement of a phantom with known concentration, where detected with the NIRF-IVUS-optoacoustic catheter concentration is scaled to the *a priory* known value. Another limitation of the system described here is that the catheter has a size of 9F and operates at a frame rate of 0.5 Hz. Encouraged by the results of the present proof-of-concept study, we are working on further technical development of the NIRF-IVUS-optoacoustic concept that will allow *in vivo* application.

The optoacoustic modality in this tri-modal catheter serves, at the moment, only for hematocrit calibration. In future work, we will exploit the imaging potential of the optoacoustic modality, such that optoacoustic images are obtained in parallel with fluorescence and ultrasound images. Optoacoustics can image features that are not resolved well by either NIRF or IVUS, especially at greater depths.[12,14,15] For example, optoacoustics can detect fat because of its absorption peak around 930 nm, allowing the imaging of lipid-rich atherosclerotic

plaques.[13] It may be possible with the tri-modal catheter to characterize plaques and assess their risk of rupture, which may lead to prediction of coronary events.

The integration of optoacoustics into a tri-modal NIRF-IVUS-optoacoustic catheter will allow much more accurate fluorescence imaging for many catheter-based clinical procedures. It creates new opportunities, such as studying plaque pathogenesis and destabilization, which may ultimately improve the assessment of plaque rupture risk and aid in the monitoring of treatment response. The possibility of operating the optoacoustic modality in mono- or multispectral mode in this tri-modal catheter may allow the analysis of various pathophysiologies in basic and translational research.

Acknowledgements The research leading to these results has received funding from the European Union Seventh Framework Programme (FP7/2007–2013) under the CosmoPHOS-nano Project, grant agreement no 310337. We acknowledge the support from the Deutsche Forschungsgemeinschaft (DFG), Germany (Leibniz Prize 2013; NT 3/10-1).

References

[1] M. Abran, B.E. Stähli, N. Merlet, T. Mihalache-Avram, M. Mecteau, E. Rhéaume, D. Busseuil, J.-C. Tardif, F. Lesage, Validating a bimodal intravascular ultrasound (IVUS) and near-infrared fluorescence (NIRF) catheter for atherosclerotic plaque detection in rabbits, Biomed. Opt. Express. 6 (2015) 3989. doi:10.1364/BOE.6.003989.

[2] A.K. Thukkani, F. a Jaffer, Intravascular near-infrared fluorescence molecular imaging of atherosclerosis., Am. J. Nucl. Med. Mol. Imaging. 3 (2013) 217–31. http://www.pubmedcentral.nih.gov/articlerender.fcgi?artid=3627519&tool=pmcentrez&rendertype=abstract (accessed May 2, 2017).

[3] D. Bozhko, E.A. Osborn, A. Rosenthal, J.W. Verjans, T. Hara, S. Kellnberger, G. Wissmeyer, S. V. Ovsepian, J.R. McCarthy, A. Mauskapf, A.F. Stein, F.A. Jaffer, V.

Ntziachristos, Quantitative intravascular biological fluorescence-ultrasound imaging of coronary and peripheral arteries *in vivo*, Eur. Hear. J. – Cardiovasc. Imaging. (2016) jew222. doi:10.1093/ehjci/jew222.

[4] E. Aikawa, M. Nahrendorf, D. Sosnovik, V.M. Lok, F.A. Jaffer, M. Aikawa, R. Weissleder, Multimodality Molecular Imaging Identifies Proteolytic and Osteogenic Activities in Early Aortic Valve Disease, Circulation. 115 (2007) 377–386. doi:10.1161/CIRCULATIONAHA.106.654913.

[5] J. Chen, C.-H. Tung, U. Mahmood, V. Ntziachristos, R. Gyurko, M.C. Fishman, P.L. Huang, R. Weissleder, In vivo imaging of proteolytic activity in atherosclerosis., Circulation. 105 (2002) 2766–71. http://www.ncbi.nlm.nih.gov/pubmed/12057992 (accessed May 2, 2017).

[6] R.Y. Khamis, K.J. Woollard, G.D. Hyde, J.J. Boyle, C. Bicknell, S.-H. Chang, T.H. Malik, T. Hara, A. Mauskapf, D.W. Granger, J.L. Johnson, V. Ntziachristos, P.M. Matthews, F.A. Jaffer, D.O. Haskard, Near Infrared Fluorescence (NIRF) Molecular Imaging of Oxidized LDL with an Autoantibody in Experimental Atherosclerosis., Sci. Rep. 6 (2016) 21785. doi:10.1038/srep21785.

[7] A. Mojsilović, M. Popović, N. Amodaj, R. Babić, M. Ostojić, Automatic segmentation of intravascular ultrasound images: a texture-based approach., Ann. Biomed. Eng. 25 (1997) 1059–1071. doi:10.1007/BF02648131.

[8] E.G.P. Bovenkamp, J. Dijkstra, J.G. Bosch, J.H.C. Reiber, Multi-agent segmentation of IVUS images, Pattern Recognit. 37 (2004) 647–663. doi:10.1016/j.patcog.2003.09.015.

[9] G. Mallas, D.H. Brooks, A. Rosenthal, R.N. Nudelman, A. Mauskapf, F. a Jaffer, V. Ntziachristos, Improving quantification of intravascular fluorescence imaging using structural information, Phys. Med. Biol. 57 (2012) 6395–6406. doi:10.1088/0031-9155/57/20/6395.

[10] B. Wang, A. Karpiouk, D. Yeager, J. Amirian, S. Litovsky, R. Smalling, S. Emelianov,

Intravascular photoacoustic imaging of lipid in atherosclerotic plaques in the presence of luminal blood, Opt. Lett. 37 (2012) 1244. doi:10.1364/OL.37.001244.

[11] P. Wang, T. Ma, M.N. Slipchenko, S. Liang, J. Hui, K.K. Shung, S. Roy, M. Sturek, Q. Zhou, Z. Chen, J.-X. Cheng, High-speed Intravascular Photoacoustic Imaging of Lipid-laden Atherosclerotic Plaque Enabled by a 2-kHz Barium Nitrite Raman Laser, Sci. Rep. 4 (2014) 6889. doi:10.1038/srep06889.

[12] J. Zhang, S. Yang, X. Ji, Q. Zhou, D. Xing, Characterization of lipid-rich aortic plaques by intravascular photoacoustic tomography: Ex vivo and in vivo validation in a rabbit atherosclerosis model with histologic correlation, J. Am. Coll. Cardiol. 64 (2014) 385–390. doi:10.1016/j.jacc.2014.04.053.

[13] K. Jansen, M. Wu, A.F.W. van der Steen, G. van Soest, Photoacoustic imaging of human coronary atherosclerosis in two spectral bands, Photoacoustics. 2 (2014) 12–20. doi:10.1016/j.pacs.2013.11.003.

[14] Y. Cao, J. Hui, A. Kole, P. Wang, Q. Yu, W. Chen, M. Sturek, J.-X. Cheng, High-sensitivity intravascular photoacoustic imaging of lipid–laden plaque with a collinear catheter design, Sci. Rep. 6 (2016) 25236. doi:10.1038/srep25236.

[15] M. Abran, G. Cloutier, M.-H.R.H.R. Cardinal, B. Chayer, J.-C.C. Tardif, F. Lesage, Development of a photoacoustic, ultrasound and fluorescence imaging catheter for the study of atherosclerotic plaque, IEEE Trans. Biomed. Circuits Syst. 8 (2014) 696–703. doi:10.1109/TBCAS.2014.2360560.

[16] K. Tohda, H. Lu, Y. Umezawa, M. Gratzl, Optical detection in microscopic domains. 2. Inner filter effects for monitoring nonfluorescent molecules with fluorescence, Anal. Chem. 73 (2001) 2070–2077. doi:10.1021/ac001030n.

[17] V. Twersky, Absorption and multiple scattering by biological suspensions., J. Opt. Soc. Am. 60 (1970) 1084–1093. doi:10.1364/JOSA.60.001084.

[18] J. Ripoll, V. Ntziachristos, Quantitative point source photoacoustic inversion formulas

for scattering and absorbing media, Phys. Rev. E - Stat. Nonlinear, Soft Matter Phys. 71 (2005) 1–9. doi:10.1103/PhysRevE.71.031912.

[19] D.K. Rosenthal, Rabbit Reference Ranges, (2003). http://cal.vet.upenn.edu/projects/ssclinic/refdesk/rabbitrr.htm.

[20] M. Suckow, K. Stevens, R. Wilson, The Laboratory Rabbit, Guinea Pig, Hamster, and Other Rodents, Elsevier, 2012. doi:10.1016/C2009-0-30495-X.

[21] R.O. Esenaliev, I. V. Larina, K. V. Larin, D.J. Deyo, M. Motamedi, D.S. Prough, Optoacoustic technique for noninvasive monitoring of blood oxygenation: a feasibility study, Appl. Opt. 41 (2002) 4722. doi:10.1364/AO.41.004722.

[22] I.Y. Petrova, R.O. Esenaliev, Y.Y. Petrov, H.-P. Brecht, C.H. Svenson, J. Olsson, D.D. Deyo, D.S. Prough, Optoacoustic monitoring of blood hemoglobin concentration: a pilot clinical study, Opt. Lett. 30 (2005) 1677–1679.

[23] Z. Li, H. Li, Z. Zeng, W. Xie, W.R. Chen, Determination of optical absorption coefficient with focusing photoacoustic imaging, J. Biomed. Opt. 17 (2012) 61216. doi:10.1117/1.JBO.17.6.061216.

[24] A. Roggan, M. Friebel, K. Do Rschel, A. Hahn, G. Mu Ller, Optical Properties of Circulating Human Blood in the Wavelength Range 400-2500 nm., J. Biomed. Opt. 4 (1999) 36–46. doi:10.1117/1.429919.

[25] D.N. Ku, Blood Flow in Arteries, Annu. Rev. Fluid Mech. 29 (1997) 399–434. doi:10.1146/annurev.fluid.29.1.399.

[26] M. Koch, V. Ntziachristos, Advancing Surgical Vision with Fluorescence Imaging, Annu. Rev. Med. 67 (2016) 153–164. doi:10.1146/annurev-med-051914-022043.

Figure 1. Schematic diagram of the tri-modal NIRF-IVUS-optoacoustic system for fluorescence, ultrasound and optoacoustic imaging. The inset is a photograph showing the NIRF-IVUS-optoacoustic catheter carrying two laser beams (pulsed 515 nm illumination is visible) to stimulate the two forms of emission from the sample. Col., collimator; CW, continuous wave; Dich., dichroic; US, ultrasound.

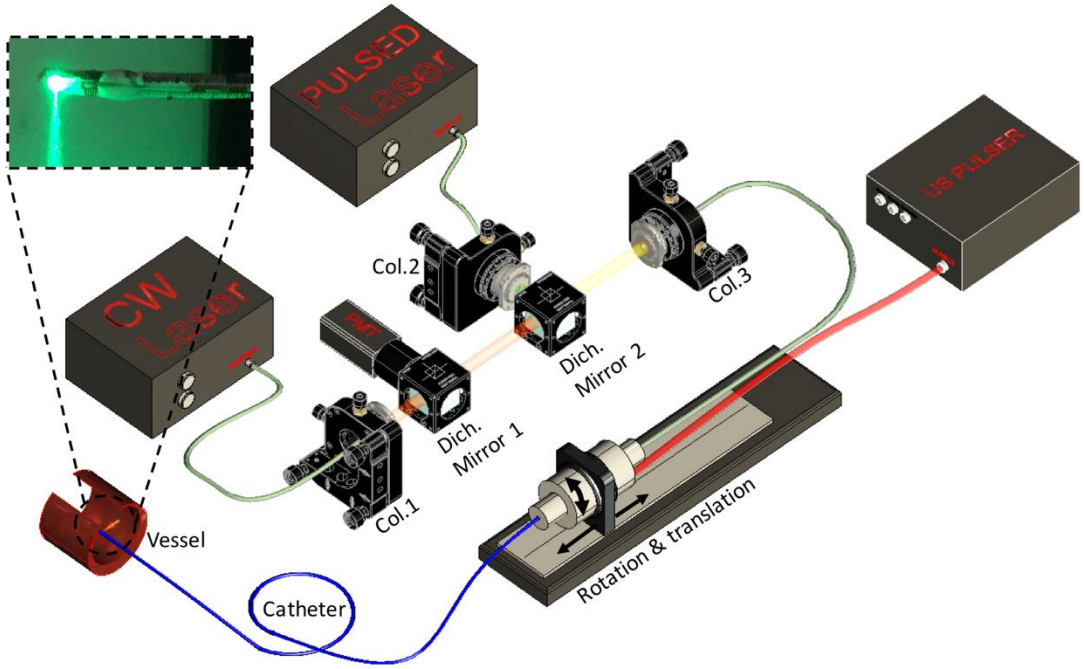

Figure 2. Development of a blood attenuation model to correct NIRF intensity. **(a)** The experimental model allows estimation of fluorophore concentration from NIRF intensity corrected based on the distance from catheter tip to fluorescent target and calibrated for hematocrit (HCT) based on the maximal optoacoustic signal (OA). **(b)** Normalized experimental NIRF intensities and two-component exponential fits as a function of distance measured in blood at different hematocrits from 0 (water) to 40% (undiluted blood). **(c)** Amplitude of optoacoustic signal generated in blood with different hematocrits. Error bars depict standard deviation over 4-6 optoacoustic measurements in phantom and ex vivo vessel.

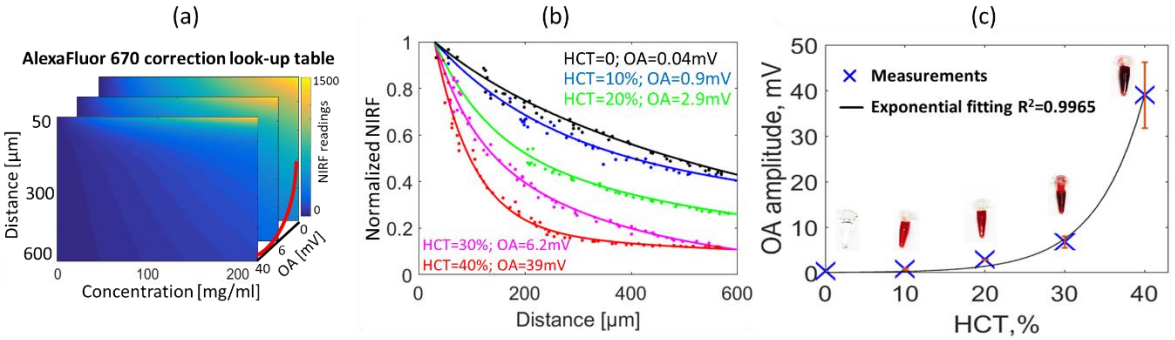

Figure 3. Phantom validation of the blood attenuation model. A fluorescent tube phantom was submerged in blood at a hematocrit of 30%. **(a)** NIRF data recorded during pullback were reconstructed without any attenuation correction**, (b)** with distance correction**,** or **(c)** with distance correction and hematocrit calibration. **(d)** Normalized NIRF signal and recovered fluorophore concentration as a function of catheter-tube distance without blood attenuation

correction (blue), with distance correction only (green), or with both distance correction and hematocrit calibration (red).

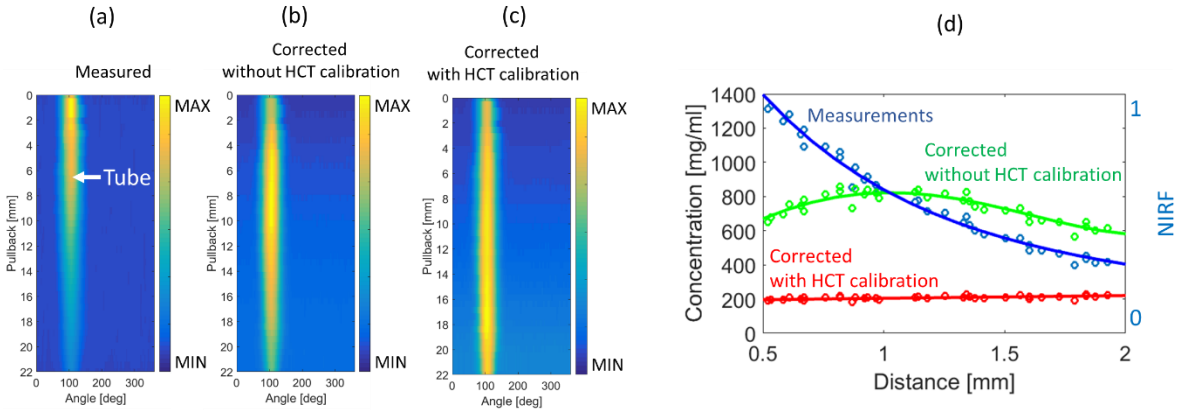

Figure 4. Validation of the blood attenuation model with abdominal rabbit aorta *ex vivo*. The aorta was injected at three sites with AlexaFluor® 680 and immersed in blood diluted to a hematocrit of 30%. **(a)** Representative tri-modal cross-sectional image. Arrow 1 indicates the vessel wall; arrow 2, a catheter sheath; and arrow 3, the edge of the blood bath in which the aorta was submerged. Inset depicts maximum intensity projection (MIP) of the optoacoustic signal over the pullback. Blue and green circles outline optoacoustic focal range 0.95-1.3 mm. Scalebar 1mm. **(b)** NIRF image of the vessel following distance correction without hematocrit calibration and **(c)** with hematocrit calibration. Red dashed circles indicate injection points. **(d)** Normalized NIRF signal and recovered fluorophore concentration as a function of pullback position without any blood attenuation correction (blue), with distance correction only (green) or with both distance correction and hematocrit calibration (red).

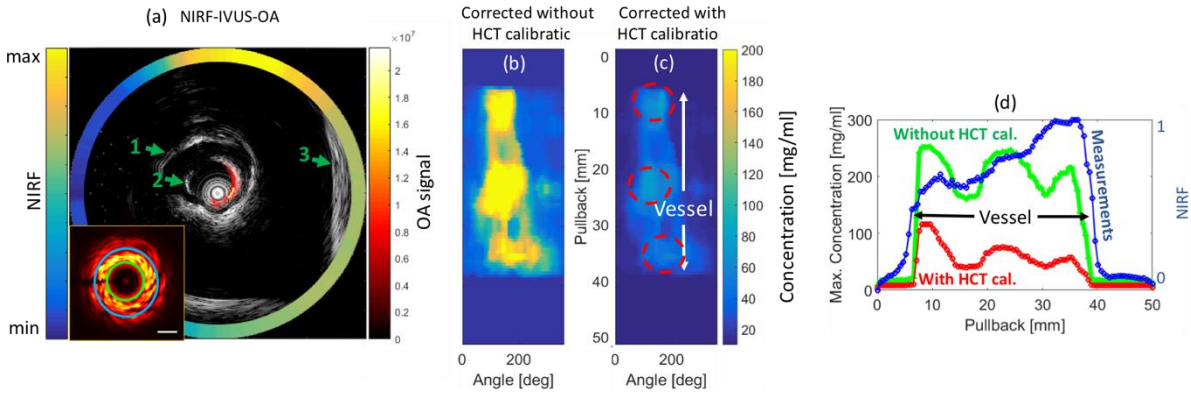

Graphical Abstract

Novel approach of absorption correction for intravascular optical imaging through blood is proposed. Using the NIRF-IVUS-optoacoustic catheter, measurements in phantoms and excised rabbit aortas are performed. Optoacoustic excitation is combined with fluorescence. Measurements are shown to determine variations of blood absorption, leading to accurate correction and quantification of the detected NIRF signals at different hematocrit values.

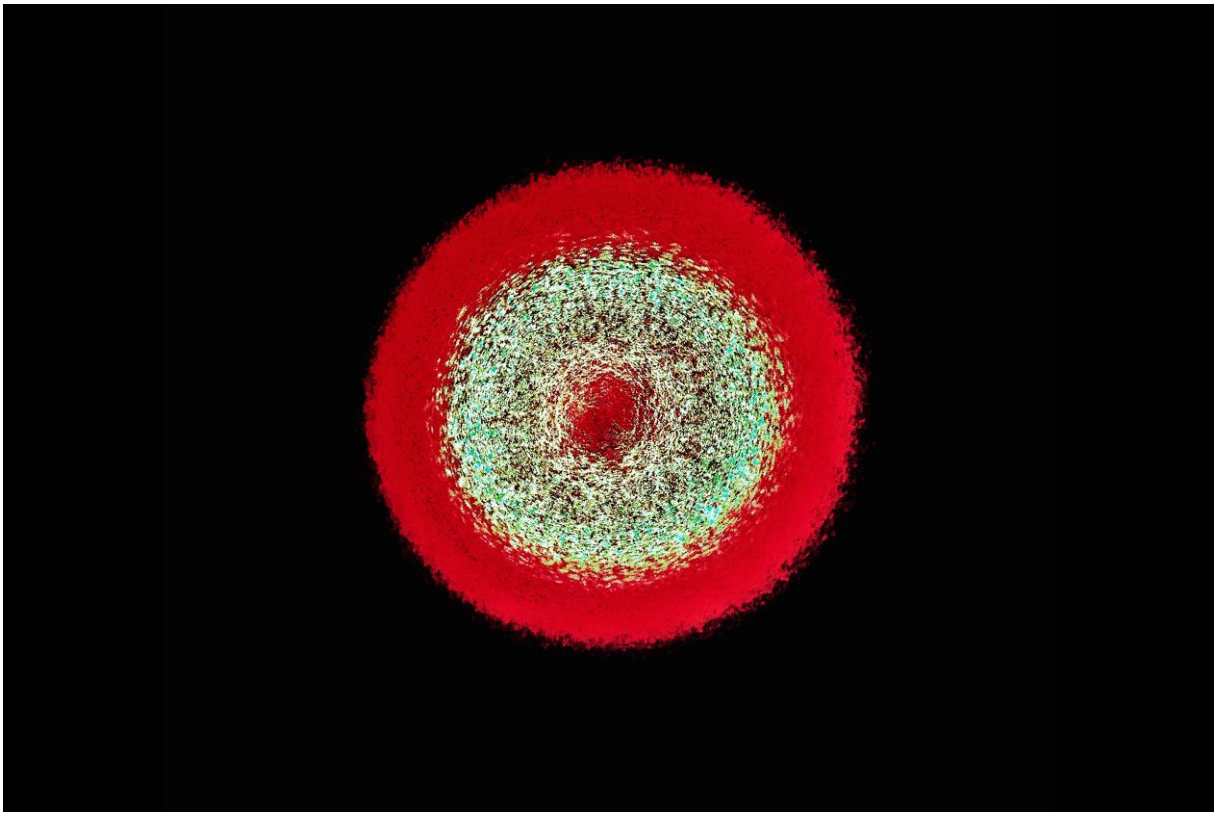

Dmitry Bozhko received his Bachelor's and Master's degrees in Radio Physics from the Peter the Great St. Petersburg Polytechnic University in Russia. Following "Stipendienprogramm Ost" fellowship from the Technical University of Munich (TUM) he started pursuing his Ph.D. in Electrical and Computer Engineering at the Chair for Biological Imaging (CBI) at TUM and the Institute for Biological and Medical Imaging (IBMI) at the Helmholtz Zentrum München. His expertise is focused in the field of intravascular imaging, medical hardware development, signal and image processing.

Angelos Karlas studied Medicine and Electrical and Computer Engineering at the Aristotle University of Thessaloniki, Greece. He holds a Master of Science in Medical Informatics from the Aristotle University of Thessaloniki, Greece, as well as, a Master of Research in Medical Robotics and Image Guided Intervention from Imperial College London, UK. He worked as a clinical resident at the 1st Department of the Rechts der Isar University Hospital in Munich, Germany. Currently, he is the Group Leader of the Clinical Multispectral Optoacoustic Tomography Group at the Institute for Biological and Medical Imaging (IBMI), Munich, Germany while pursuing his PhD (Dr.rer.nat.) in Experimental Medicine at the Technical University of Munich, Germany. His main research

interests include optical and optoacoustic molecular imaging techniques with applications to the cardiovascular system and metabolism.

Dr. Dimitris Gorpas is a senior scientist at Department of Biological Imaging (CBI) at Technical University of Munich and the Insitute of Biological and Medical Imaging (IBMI) at Helmholtz Zentrum München and is leading the Fluorescence Imaging group. He received his PhD in engineering from the National Technical University of Athens, Greece, and was a postdoctoral fellow in biomedical engineering at the University of California, Davis, USA. He has extensive experience in medical image and signal processing, surface three-dimensional reconstruction and modelling of light/matter interaction, and software and hardware development. His research mainly focuses in the development of new analysis techniques to aid the detection and monitoring of in vivo molecular processes associated with cancer or other diseases.

Vasilis Ntziachristos Ph.D. is Professor and Chair for Biological Imaging at the Technical University of Munich and Director of the Institute of Biological and Medical Imaging at the Helmholtz Zentrum München. Prior to this appointment, he was faculty at Harvard University and the Massachusetts General Hospital. He received his masters and doctorate degrees from the Bioengineering Department of the University of Pennsylvania and the Diploma in Electrical Engineering from the Aristotle University of Thessaloniki, Greece. Professor Ntziachristos serves as chair in international meetings and councils and in the editorial boards of several scientific journals. He has received numerous awards and distinctions, including the Leibniz prize of the German Research Association (DFG, 2013), the Gold Medal of the World Molecular Imaging Society (WMIS, 2015), and two Advanced Investigator Awards from the European Research Council (ERC, 2008 and 2016). His main research interests focus on advancing optical and opto-acoustic imaging techniques for biomedical discovery with a strong drive toward clinical translation.

SUPPLEMENTAL MATERIAL

Optoacoustic sensing of hematocrit to improve the accuracy of hybrid fluorescence-ultrasound intravascular imaging

Dmitry Bozhko,[1,2], Angelos Karlas[1,2], Dimitris Gorpas[1,2] and Vasilis Ntziachristos[1,2,]*

*Corresponding Author: E-mail: v.ntziachristos@tum.de

[1] Institute of Biological and Medical Imaging, Helmholtz Zentrum München, Neuherberg, 85764 Germany

[2] Chair of Biological Imaging, Technische Universität München, Munich, 85764 Germany

SUPPLEMENTAL RESULTS

In Experiment 1 we measured the NIRF signal as function of distance in blood diluted to hematocrit levels of 0, 10%, 20%, 30%, and 40%. We normalized experimental data and, as per Twersky theory,[17] fitted it with two-term exponential functions of the form

$$\mathrm{NIRF}(\mathrm{dist}) = \mathrm{a} * \exp(\mathrm{b} * \mathrm{dist}) + \mathrm{c} * \exp(\mathrm{d} * \mathrm{dist}),$$

where NIRF is detected fluorescence signal, dist – distance between the catheter and the tube in μm., a,b,c, and d are used fitting parameters which we show in **Table 1**.

Measured relationship between optoacoustic amplitude and hematocrit was fitted with a single-term exponential function. Parameters are presented in **Table 1**.

Parameters	a	b	c	d
HTC=40%	1.232	-0.01361	0.1858	-0.00091
HTC=30%	0.6054	-0.01443	0.6653	-0.00304
HTC=20%	0.6243	-0.00938	0.5493	-0.00127
HTC=10%	0.579	-0.00452	0.5024	-0.00053
HTC=0	0.1414	-0.00673	0.9191	-0.00128
OA signal	0.0362	0.06981	0	0

Table 1. Fitting parameters for the developed correction model.